X-ray diffractometer designed for industrial applications at SPring-8 BL24XU

Etsuya Yanase,* Konstantin Vladimirovich Zolotarev, Kozi Nishio, Yukihiro Kusumi, Hideki Okado and Kazuo Arai

The New Industry Research Organization, 1-5-2, Minatojima-minamimachi, Chuo-ku, Kobe, 650-0047, Japan. E-mail: yanase@ri.niro.or.jp

An X-ray diffractometer for industrial applications has been designed, installed at SPring-8 BL24XU and tested by measuring a standard Al_2O_3 powder sample. The measurement results prove the high precision of the diffractometer. The diffractometer was also tested by conducting grazing-incidence X-ray diffraction measurements of ion-implanted chromium-coated steel. The validity of a new method for X-ray stress measurements of polished stainless steel is also proposed and confirmed. The results prove the suitability of this diffractometer for industrial applications.

Keywords: X-ray diffractometers; industrial applications; grazing-incidence X-ray diffraction; stress measurement; ion implantation.

1. Introduction

X-ray analysis is an established on-site technology in various industrial fields. X-ray analysis is also used in the research and development of new products. A new X-ray source, synchrotron radiation, has now become the center of attention because it provides wavelength variability and ultra-bright highly directional beams. Thanks to these properties, synchrotron radiation is expected to contribute greatly not only to research but also to quality control.

Material surface preparation and modification are excellent ways of improving material properties and production properties. Surface treatment can increase material hardness, decrease the coefficient of friction and impart increased resistance to wear and corrosion. However, the quality of these useful surface properties depends on crystal structure, residual stress and chemical composition. Therefore, being able to analyze and evaluate these factors is essential for quality control and quality assurance. X-ray analysis, especially that using synchrotron radiation as the X-ray source, has specific advantages and provides specific data that cannot be obtained with other surface-analysis techniques. Focusing our attention on the use of grazing-incidence X-ray diffraction and X-ray stress analysis for industrial applications, we designed an X-ray diffractometer that has been installed at SPring-8 BL24XU in Japan.

Hyogo beamline BL24XU (Matsui *et al.*, 1998) at SPring-8 was constructed for the purpose of protein crystal structure analysis, surface/interface analysis of inorganic materials, X-ray microbeam analysis (Tsusaka *et al.*, 2000) and the development of X-ray imaging (Kagoshima *et al.*, 2000). To be able to perform these activities simultaneously, this beamline has three experimental hutches (A, B, C) in a 'troika' arrangement; it has diamond monochromators and employs a 'figure-8' undulator (Tanaka & Kitamura, 1995). We installed our X-ray diffractometer for material analysis in hutch B. In this paper, we describe the design of the diffractometer and report the results of tests to establish its performance.

Table 1
Diffractometer performance.

	Stage	Range	Minimal step	Load (kg)
Base stages	α	±3°	0.144"	2000
	Base X	±50 mm	0.11 μm	2000
	Base Z	−80–20 mm	1 μm	2000
Sample stages	x, y	±10 mm	0.5 μm	10
	z	±10 mm	1 μm	15
	Φ	±180°	1.8"	20
	χ	0–90°	0.288"	50
	ω	−20–100°	0.144"	110
Detector stages	2θ	−100–80°	0.288"	100
	δ	±5°	7.2"	7
	X_δ	−10–50 mm	1 μm	25

2. Diffractometer design

Fig. 1 shows a photograph of the X-ray diffractometer. The design is based on a conventional four-circle diffractometer called an Eulerian cradle type. The diffractometer has been designed to allow grazing-incidence X-ray diffraction (GIXRD) experiments and residual stress measurements of industrial materials. Because it is intended for industrial applications, the maximum load of the sample stages was designed to be 10 kg so that various apparatuses can be placed on the stages for controlling the sample environment. The dimensions of the free space available for the sample and its environment are 250 × 250 × 250 mm. With a view to measuring residual stress, the χ measuring circle has a gap through which diffraction peaks with a high Bragg angle can be detected. Moreover, the ω circle stage has a hole on each side so that an X-ray fluorescence detector can be installed in the future.

The performance of each axis is summarized in Table 1. The diffractometer system has six rotation stages and six linear stages, which can be divided into three groups. The first group consists of the base stages, which can adjust the center of the goniometer on the X-ray beam. The second consists of the sample stages, which can also

Figure 1
Photograph of the X-ray diffractometer at SPring-8 BL24XU.

 © 2002 International Union of Crystallography • Printed in Great Britain – all rights reserved

center the goniometer. The third group consists of the detector stages, which can drive an X-ray detector. The geometry of the stages is shown schematically in Fig. 2. The sample placed on the x, y and z linear stages is mounted on the Φ rotation stage.

When GIXRD measurement is carried out, the sample must be placed on the stage vertically because the X-ray beam supplied at BL24XU has horizontal polarization. Therefore, the sample and detector stages are rotated using the α stage and Φ stage for incidence at a grazing angle on the sample surface. For residual stress measurements, a sample can be rotated around the ω axis or the χ axis for each stage using the iso-inclination mode (Ω diffractometer method) or the side-inclination mode (Ψ diffractometer method), respectively.

A scintillation counter or a one-dimensional position-sensitive proportional counter (PSPC) can be mounted on the 2θ arm as an X-ray detector. A scintillation counter is mounted on an optical rail with slits made of four independent blades and a helium path for suppressing air-scattered X-rays. This rail can be driven by the δ rotational stage and X_δ linear stage. Furthermore, the maximum load of the 2θ arm stage has been designed to be 100 kg so that Soller slits or a crystal analyzer can be installed in the future.

A PSPC detector (Aulchenko *et al.*, 1998) is available for *in situ* measurements or for saving time. The performance characteristics of this detector are listed in Table 2. Because this PSPC detector is curved, it is important to adjust the center of the goniometer on the focal point. This adjustment is carried out with a tile angle of the equipment on which the detector is mounted.

3. Test materials and methods

The diffractometer was installed and tested at SPring-8 BL24XU in Japan, and then it was used for making measurements of some industrial materials. The X-ray beam used for these measurements was monochromated to about 10 keV by a diamond (220) crystal. The incident beam intensity was monitored with an ionization chamber, and the diffraction beam was detected by a scintillation counter. The beam size, 0.4 mm wide and 0.1 mm high, was controlled by the set of slits composed of four independent blades upstream of the incident X-ray monitor.

To evaluate the performance of the diffractometer, we measured the X-ray diffraction pattern of a NIST standard Al_2O_3 powder sample (standard reference material 674*a*). The Al_2O_3 powder sample was placed on a typical glass plate holder for an X-ray diffractometer. We used a collimator placed on the χ stage to adjust the center of the goniometer on the X-ray beam. This collimator has a pinhole that is adjusted to the center of the goniometer in advance. The X-ray beam passing through this collimator is detected by an ionization chamber downstream of the collimator with driving base X stage and Z stage.

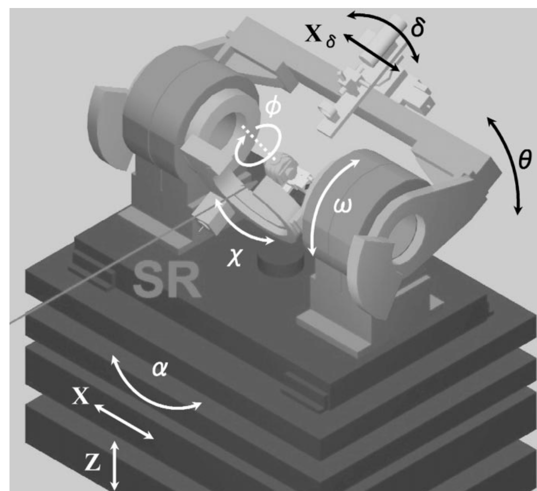

Figure 2
Schematic view of the X-ray diffractometer.

Table 2
PSPC detector performance.

X-ray window	Be (200 × 10 × 0.2 mm)
Available angle	30°
Curved radius	350 mm
Scale	3300 channels
Channel width	0.01° (60 μm)
Angle resolution (FWHM)	0.05°
Maximum frame number	1024
Frame time	1 μs–1024 s
Count rate (50% loss)	10^6 events s^{-1}
Energy range	5–20 keV

Chromium-coated steel and polished stainless steel were used as test samples of industrial materials.

Chromium-coated steel with nitrogen or fluorine ions implanted is used in molds for rubber products to prevent adherence in the molding process. The surface structure modified by nitrogen ion implantation and by fluorine ion implantation (30 keV energy) was analyzed by GIXRD measurement.

Polished stainless steel, in which internal stress is distributed on the surface by polishing with emery paper, was measured to confirm the validity of our new stress-analysis method. This method may be said to be a mixture of the iso-inclination and side-inclination modes. It makes it possible to measure the $\sin^2\psi$ diagrams while maintaining the incident angle. The incident angle α is given by the following equation when the χ and ω axes of our diffractometer are used,

$$\sin\alpha = \cos\chi\sin\omega. \tag{1}$$

The ψ angle in the $\sin^2\psi$ mode is given by the following equation,

$$\cos\psi = \cos\chi\cos(\theta_0 - \omega). \tag{2}$$

These equations demonstrate that we can measure $\sin^2\psi$ diagrams while maintaining the incident angle, or, in other words, almost without changing the probing depth. The details of this new method have been described elsewhere (Yanase *et al.*, 2001).

4. Results and discussion

We measured the X-ray diffraction patterns of a powder sample with our diffractometer. In order to estimate the performance of the diffractometer, the differences between the observed Bragg angles $\delta\theta$ and those calculated using lattice parameters a = 0.4759397 nm and c = 1.299237 nm are shown in Fig. 3. The differences were caused mainly by deflection of the goniometer center. We estimated this deflection distance S using the following equation (Kohra *et al.*, 1963),

$$\delta\theta = A + (2S/R)\cos\theta + B\sin 2\theta, \tag{3}$$

where A and B are fitting parameters and R is the radius of the goniometer (R = 415 mm). The cosine term indicates deflection and the sine term indicates systematic error. After the fitting procedure we obtained the following values,

$S = 0.01978 \pm 0.01796$,
$A = 0.00031 \pm 0.00011$,
$B = -0.00037 \pm 0.00004$.

Because the S value is in millimeters, the deviation distance can be estimated to be not more than 20 µm. This value is sufficiently small, because it is difficult to reduce the value any further in view of mechanical accuracy.

Fig. 4 shows the results of grazing-incidence X-ray diffraction of the chromium coating implanted with nitrogen ions. The diffraction patterns indicate that the sample's surface layer was formed of chromium nitrides. These chromium nitrides were determined to be mostly CrN, with some Cr_2N also present. In the diffraction patterns of the chromium coating implanted with fluorine ions, shown in Fig. 5, there were no diffraction peaks other than those of metallic chromium. This suggests that fluorine is implanted between the atoms of the metallic chromium crystals or that the reaction product of fluorine and chromium is either amorphous or a microcrystal.

We obtained a $\sin^2\psi$ diagram of a polished stainless steel sample using the conventional iso-inclination method. The results are shown in Fig. 6. The dispersion of data was caused by the lack of measurement time. However, this diagram clearly shows nonlinearity, especially at the higher ψ angles, because the specimen had stress distributed on the surface. Next, we obtained a $\sin^2\psi$ diagram of the same specimen using our new method. For the measurements, we used $\alpha = 2$, 3, 5 and 7° as the X-ray incident angle. The results are shown in Fig. 7. Although the diagram in Fig. 6 showed strong nonlinearity, the lines plotted in Fig. 7 are almost straight. This verifies that our new method is applicable to stress measurement of a specimen with stress gradients.

5. Conclusions

We designed an X-ray diffractometer for industrial applications and installed it at SPring-8 BL24XU in Japan. We measured the X-ray diffraction peaks of a standard NIST Al_2O_3 powder sample and obtained satisfactory results. Next, the diffractometer was used for the grazing-incidence X-ray diffraction measurement of ion-implanted chromium-coated samples and for the X-ray stress measurement of polished stainless steel using our proposed new method. The results proved the validity of our diffractometer for industrial applications, and we look forward to this diffractometer being put to use for many industrial applications.

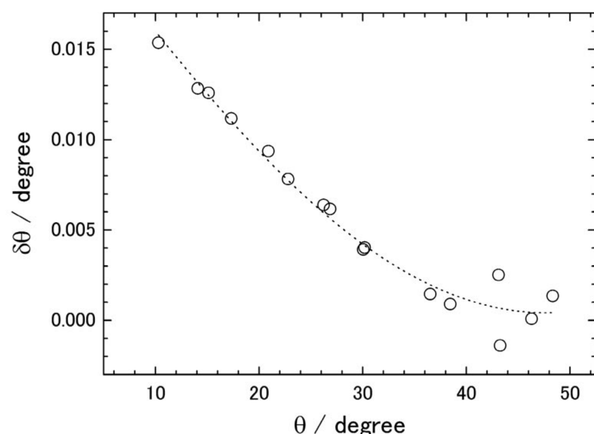

Figure 3
Differences between calculated and observed Bragg angle. The broken line is a fitted curve.

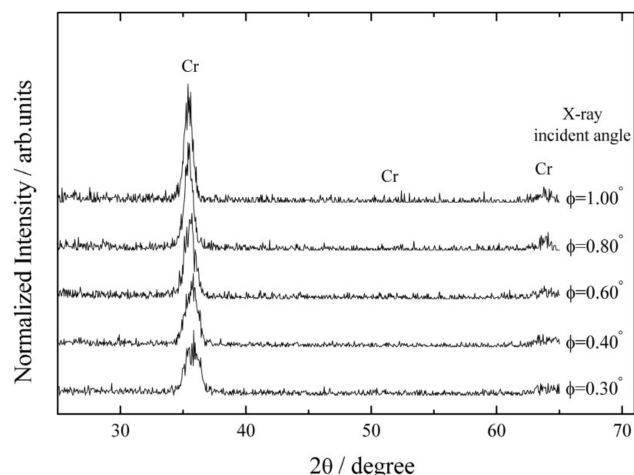

Figure 5
Diffraction patterns of fluorine-ion-implanted (30 keV energy) chromium coating measured using grazing-incident X-ray diffraction. Φ angles are X-ray incident angles.

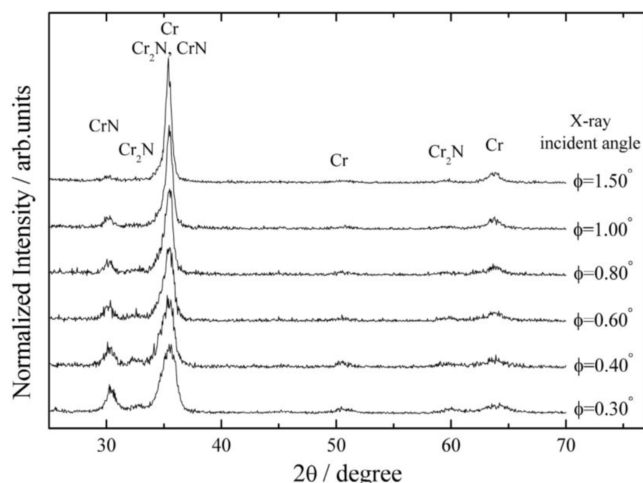

Figure 4
Diffraction patterns of nitrogen-ion-implanted (30 keV energy) chromium coating measured using grazing-incident X-ray diffraction. Φ angles are X-ray incident angles.

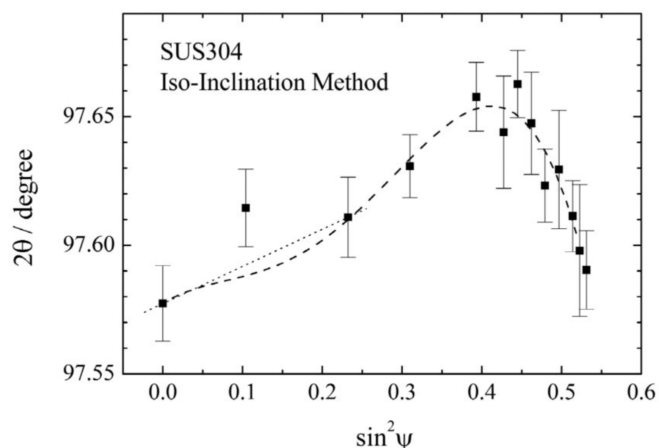

Figure 6
$\sin^2\psi$ diagram of a stainless steel sample measured by the iso-inclination method.

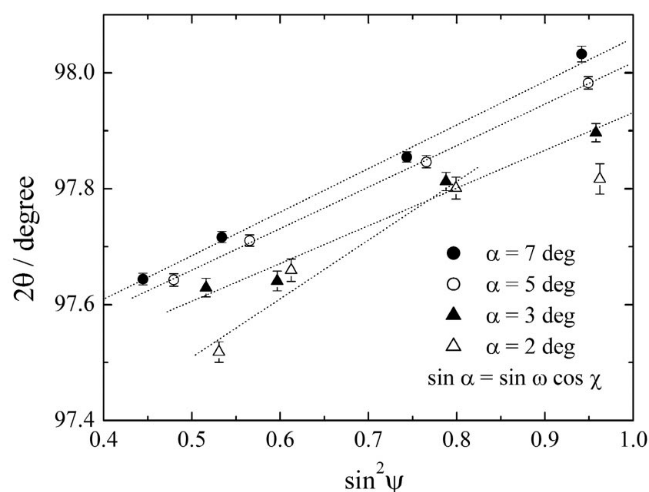

Figure 7
$\sin^2\psi$ diagram of a stainless steel sample measured by our new method. α angles are X-ray incident angles.

This project was conducted under the approval of the JASRI (Proposal No. C99B24XU-535N, C00A24XU-535N). The authors are indebted to the Ion Engineering Research Institute Corporation for its financial support of this research through the Special Coordination Funds received from New Energy and Industrial Technology for promoting the industrial production by local consortiums of the project entitled 'Development of High-Quality Low-Cost Dies for Rubber and Plastic Molding'.

References

Aulchenko, V. M., Bukin, M. A., Velikzhanin, Yu. S., Gaponenko, Ya. V., Dubrovin, M. S., Titov, V. M., Ancharov, A. I., Gaponov, Yu. A., Evdokov, O. V., Tokochko, B. P. & Sharafutdinov, M. R. (1998). *Nucl. Instrum. Methods*, A**405**, 269–273.

Kagoshima, Y., Ibuki, T., Takai, K., Yokoyama, Y., Miyamoto, N., Tsusaka, Y. & Matsui, J. (2000). *Jpn J. Appl. Phys.* **39**, L433–435.

Kohra, K., Hoyoya, S., Doi, K. & Niizeki, N. (1963). *Xsenn Kessyougaku no riron to jissai*, Second Edition (In Japanese), p. 187. (Translation of *Théorie et Technique de la Radiocristallographie*, André Guiner.)

Matsui, J., Kagoshima, Y., Tsusaka, Y., Katsuya, Y., Motoyama, M., Watanabe, Y., Yokoyama, K., Takai, K., Takeda, S. & Chikawa, J. (1998). *SPring-8 Annual Report 1997*, pp. 125–130. SPring-8, Hyogo, Japan.

Tanaka, T. & Kitamura, H. (1995). *Nucl. Instrum. Methods*, A**364**, 368–373.

Tsusaka, Y., Yokoyama, K., Takeda, S., Urakawa, M., Kagoshima, Y., Matsui, J., Kimura, S., Kimura, H., Kobayashi, K. & Izumi K. (2000). *Jpn J. Appl. Phys.* **39**, L635–637.

Yanase, E., Zolotarev, K. V., Nishio, K., Kusumi, Y., Arai, K. & Nakagawa, S. (2001). *J. Neutron Res.* **9**, 273–279.

 Received 11 March 2002 • Accepted 5 July 2002